Journal of GeoEngineering, Vol. 17, No. 1, pp. 001-010, March 2022
http://dx.doi.org/10.6310/jog.202203_17(1).1

MODELING OF SETTLEMENT AND BEARING CAPACITY OF SHALLOW FOUNDATIONS IN OVERCONSOLIDATED CLAYS

Marko Lopez [1*] and Roberto Quevedo [2]

ABSTRACT

This paper focuses on the characterization of the fine-grained soils of Pucallpa and on theoretical and numerical analyses of their bearing capacity. A review of data related with field investigation and laboratory testing is first presented aiming the assessment of geotechnical parameters for modelling the mechanical behavior of overconsolidated clays with a numerical model based on both frictional and critical state models. Considering the finite element method, several models under plane strain conditions are built for the evaluation of the ultimate bearing capacity of the soil foundation. In each model, the initial stresses used to start the simulations are obtained according to different overconsolidation ratios. Then, the ultimate bearing capacities obtained are compared with some theoretical solutions based on drained and undrained shear strengths. According to the results, the theoretical solution that considers a general shear failure mode can provide a good forecast of the ultimate bearing capacity of overconsolidated clays under drained conditions. However, depending on the allowable settlements, the bearing capacity can be significantly lowered to avoid damage to structures and buildings, even for highly overconsolidated clays.

Key words: Bearing capacity, soil settlement, shallow foundations, numerical modeling.

1. INTRODUCTION

Pucallpa is the capital of the Ucayali region (the second largest of Peru), the Coronel Portillo Province and the Calleria District. The soil stratigraphy follows a monotonous succession of some sedimentary rocks of the upper Tertiary, poorly to moderately consolidated, consisting of shales and sandstones with some intrusive calcareous layers. Such sedimentary rocks are covered by Quaternary deposits of fine-grained soils composed by clays, sands and silts. Most of those deposits are the result of transport and accumulation of sediments as well as erosion processes, typical from the Amazon plain. Several geotechnical investigations have been performed in different places of the city aiming the characterization of its soils (Alva 2013; Ramírez *et al.* 2018; Alva 2018). Some empirical correlations using the Standard Penetration Test (SPT) were used to determine the in-situ soil properties such as the unit weight and the unconfined compressive strength. In addition, soil classification, consolidation, direct shear and triaxial tests have also been carried out in laboratory considering different soil samples of Pucallpa. However, despite the data acquisition and experimental testing, most geotechnical projects performed have focussed either on the forecast of the bearing capacity of foundations or on the assessment of settlements, typical of grain-fined soils.

Since the pioneering work of Terzaghi (Terzaghi 1943), the bearing capacity of soils has been extensively studied considering theoretical models (Meyerhoff 1951; Vesic 1973; Chwala and Pula 2020). In the same way, the soil settlement has been analyzed in several studies considering settlements that develop immediately after load applications (Biot 1941; Terzaghi 1943; Mandel 1953; Gibson and Mcnamee 1963; Davis and Raymond 1965; Lee *et al.* 1992). However, such theoretical solutions are limited to several assumptions related to the soil mechanical behavior. Regarding the bearing capacity, the theoretical solutions consider foundations resting over stiff soils that after reaching a peak pressure develop a general shear failure mode. In turn, the analyses of settlements assume an elastic behavior of the soil and disregard the occurrence of plastic or viscous deformations.

Nowadays, the emergence of powerful numerical methods and computers has made it possible to overcome the limitations of the numerical modelling. For example, more comprehensive constitutive relations can be adopted to analyse more appropriately the bearing capacity of soil foundations (Liyanapathirana *et al.* 2009; Budhu 2012; Chakraborty and Kumar 2013; Tang *et al.* 2017; Kawa and Pula 2019; Rachdi *et al.* 2019). Moreover, for more realistic analyses, fully coupled hydromechanical models can be applied to assess immediate settlements as well as soil consolidation and creep (Huang *et al.* 2006; Foye *et al.* 2008; Quevedo 2012; Sun *et al.* 2014; Schneider-Muntau and Bathaeian 2018; Kristić *et al.* 2020; Radhika *et al.* 2020; Goh *et al.* 2020; Chen *et al.* 2020). However, despite the advantages of numerical modelling for geotechnical engineering design, the use of numerical tools and more comprehensive constitutive relations remain little explored in Peruvian geotechnical applications.

In this study, a review of previous and recent experimental programs performed at different places of Pucallpa is presented. The data in this work are related to site investigations (SPT) and laboratory tests (soil classification, one-dimensional consolidation and triaxial tests). After the soil characterization, the constitutive relationships of the Modified Drucker-Prager/Cap model are introduced, and the corresponding parameters are assessed. Then, numerical simulations of a shallow strip foundation are carried

Manuscript received May 6, 2021; revised September 1, 2021; accepted December 13, 2021.
[1*] Professor (corresponding author), Universidad de Lima, Instituto de Investigación Científica, Carrera de Ingeniería Civil, Perú (e-mail: mlopezb@ulima.edu.pe).
[2] Project Manager, Institute Tecgraf, Pontifical Catholic University of Rio de Janeiro, Brazil.

out using a finite element software (ABAQUS 2020). In those simulations, the initial conditions of the soil, such as its stresses, are defined as a function of the overconsolidation ratio in order to analyse their impact on both the bearing capacity and the settlement of the soil. The obtained results highlight the importance of data acquisition and the use of numerical modelling for the design of shallow foundations in Peruvian tropical regions.

2. EXPERIMENTAL PROGRAM AND SOIL CHARACTERIZATION

Several geotechnical investigations have been carried out in some places of Pucallpa aiming to characterize the soil behaviour. Figure 1 shows a map of Pucallpa city, indicating fifteen places where some field tests were performed and soil samples were collected for laboratory tests. Nine places (P-1 to P-9) correspond to previous geotechnical exploration programs reported in the literature (Díaz 2000; Alva 2013; Alva 2018) whereas the other six (P-10 to P-15) correspond to recent campaigns.

In-situ analyses were performed through SPT. In such studies, soil properties can be assessed through empirical correlations in terms of the number N required to produce a penetration of 30 cm into the soil. Figure 2(a) shows some results obtained at P-1, P-2, P-3, and P-4. It is observed a dispersion of N values ranging mainly from 8 to 40. The extreme value (N = 58) observed at a 2 m depth at P-3 is explained by the presence of high sand content found in some parts of that region (Alva 2013). Through empirical correlations (Terzaghi and Peck 1967; Hara *et al.* 1974; Ajayi and Balogum 1988), the SPT has been used to obtain different parameters for fine-grained soils such as the unconfined compressive strength (*UCS*). Figure 2(b) shows the

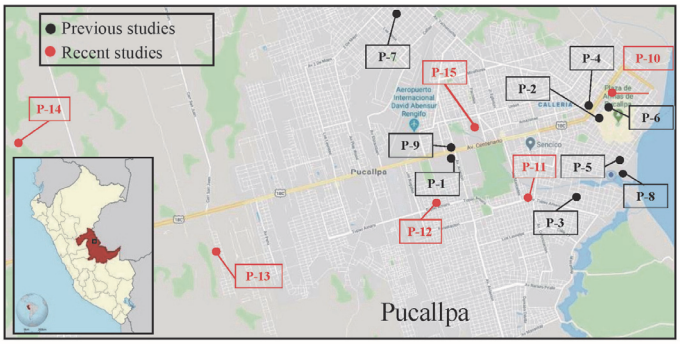

Fig. 1 Site characterization and identification of experimental programs

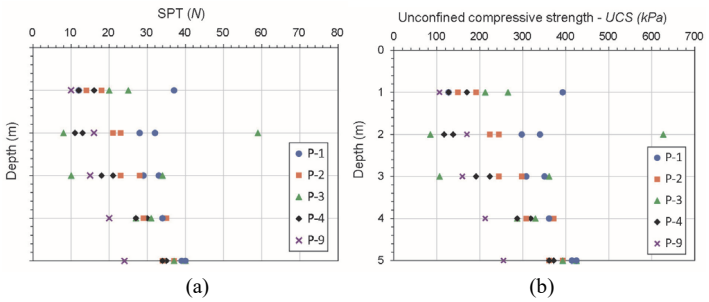

(a) (b)

Fig. 2 Field measurements along the depth: (a) SPT number and (b) unconfined compressive strength

UCS values obtained following an adapted relation given by (Terzaghi and Peck 1967) as $UCS = 12.5\ cf \times N$, where $cf = 0.85$ is a correction factor that depends on the used equipment. The obtained results indicate that the soils of Pucallpa can be classified as medium-stiff soils with *UCS* values ranging from 80 to 425 kPa.

The excavation of several pits in recent campaigns has allowed the extraction of undisturbed samples collected at 3 m depth. Figure 3(a) shows the stratigraphy at P-12. It is noted some layers of compacted clay with different colors, varying from white at the surface to red at the bottom of the pit. Cubic samples of 50 cm side were collected adopting standard procedures in order to maintain the soil's natural moisture. Then, the samples were taken to a laboratory for sample preparation and testing, as it is shown in Fig. 3(b). The measurements of moisture content provided values ranging from 10% to 45%.

The samples and the tests used for grain size analyses were prepared according to ASTM D 421 and ASTM D 422 procedures. The clay fraction was assessed as the percentage of fine grains lower than 2 μm size. The results shown in Fig. 4 correspond to samples taken from six places of Pucallpa in recent campaigns. All results indicate that the soils of Pucallpa present more than 40% of very fine grains basically composed by clays.

The Unified Soil Classification System (USCS) was adopted for soil classification. Sample preparation and tests were carried out according to ASTM D 421 and ASTM D 4318 procedures, respectively. The results are shown in Fig. 5. According to their

(a) (b)

Fig. 3 Field and laboratory: (a) site characterization at P-12 and (b) soil sample used for testing

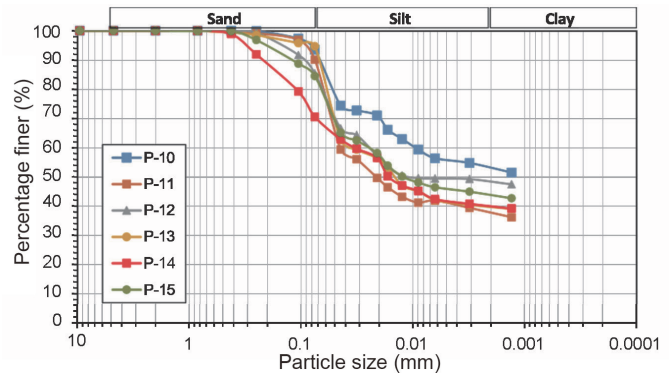

Fig. 4 Particle size distribution curves at 3 m depth in different samples of Pucallpa

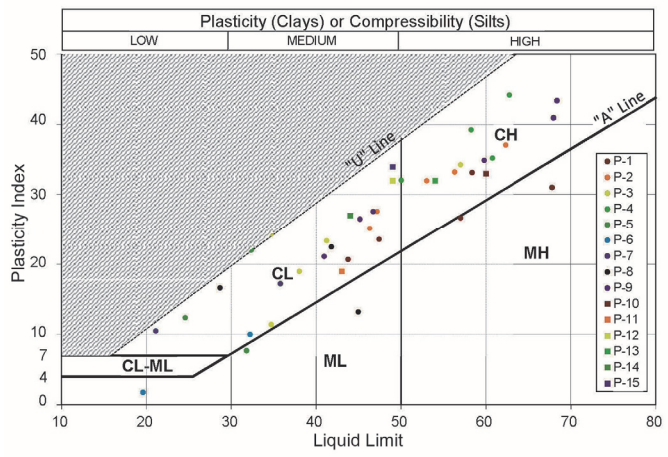

Fig. 5 Soil type according to USCS classification

liquid limits and plasticity characteristics, the fine-grained soils of Pucallpa can be categorized as clays of low (CL) and high (CH) plasticity. The liquid limit (LL) and the plasticity index (PI) range from 28 to 78 and from 10 to 55, respectively. Those limits are typical from tropical soils in South America. In Iquitos, a city near from Pucallpa, the limits are LL = 21 ~ 112 and PI = 8 ~ 73 (Bustamante and Alva 1995). Brazilian clays from Rio de Janeiro present LL = 32 ~ 60, PI = 0 ~ 8; from Goiás LL = 60 ~ 69, PI = 21 ~ 26; from Bahia LL = 78 ~ 83, PI = 67 ~ 69, and from São Paulo LL = 33 ~ 128; PI = 6 ~ 93 (Rigo *et al.* 2006). Clays of the Sabana de Bogotá in Colombia present LL = 62 ~ 65 and PI = 30 ~ 35 (Camacho and Reyes 2005).

One-dimensional consolidation tests were also carried out according to ASTM D 2435 procedure. Samples of 60 mm diameter and 20 mm height, as it is shown in Fig. 6(a), were vertically loaded and then unloaded. Figure 6(b) shows the results obtained with a sample collected from P-11 at 3 m depth. The red points are the measured experimental results, and the continues lines represent the calibrated virgin and swelling consolidation lines whose slopes define the compression (C_c) and the recompression (C_r) indices, respectively.

The first intersection between the experimental data and the virgin compression line defines the soil precompression or vertical preconsolidation stress (σ'_{v0} = 120 kPa) while the intersection between the virgin consolidation line and σ'_v = 1 kPa defines the void ratio under normal consolidation (e_{v0} = 0.61). According to Bustamante and Alva (1995), similar values

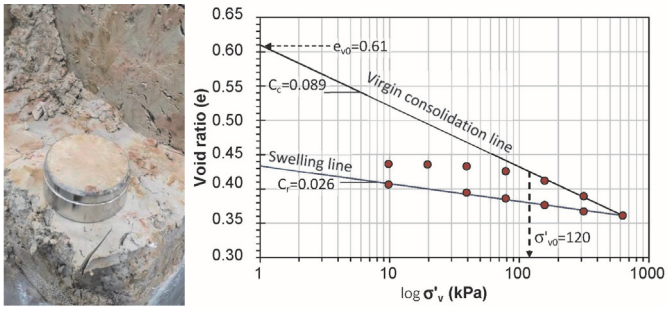

(a) (b)

Fig. 6 One-dimensional consolidation test: (a) soil sample and (b) results

can be found in Iquitos (σ'_{v0} = 1.20 ~ 2.40 kPa, e_{v0} = 0.74 ~ 1.10 and C_c = 0.14 ~ 0.28 (Bustamante and Alva 1995)). However, those soils are less compressible if compared with clays from the Postpampeano formation in Argentina and from the Sabana de Bogotá which present C_c = 0.40 (Ledesma 2007) and C_c = 0.28 ~ 0.59 (Camacho and Reyes 2005), respectively.

Triaxial tests considering soil samples collected at P-15 were carried out under drained conditions (Fig. 7(a)). Three samples with 51.7 mm diameter and 115.3 mm height were initially saturated and then confined to a certain pressure before deviatoric axial stresses were applied. The confining pressures were 100, 200, and 400 kPa. Axial compression rate of 0.1 mm/min was adopted to guarantee drained conditions. The tests were carried out until the failure of the samples was triggered or a maximum axial strain of 14% was reached. During the tests, the applied deviatoric stress (σ_d), as well as the axial and volumetric strains, were recorded. Figure 7(b) shows the obtained Mohr circles in each test. From the resultant failure envelope, it is obtained a soil cohesion (c') equal to 20 kPa and a friction coefficient (μ) equal to 0.21, which corresponds to a friction angle (ϕ') equal to 10.9°.

The reduced friction angles can be explained by the high clay content in the samples. When the clay content is greater than 50 percent, the friction angle is governed entirely by the sliding of clay minerals (Kulhawy and Mayne 1990). Therefore, a mineralogical characterization of the soil samples was performed through the X-ray diffraction with a Bruker-D8 Advance-Cobalt tube (38 kV, 25 mA). The results for a sample collected from P-10 (Table 1) show that most clay minerals are composed by muscovite and kaolinite, which can be responsible for low friction angles in overconsolidated clays (Skempton 1985).

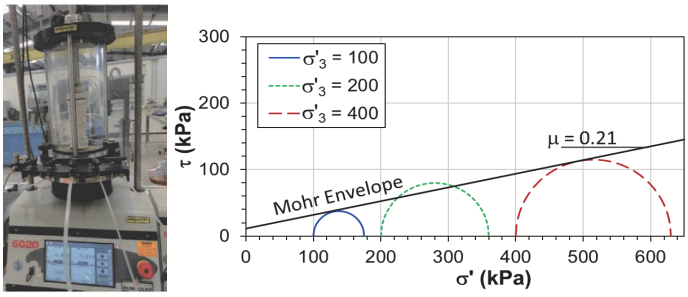

(a) (b)

Fig. 7 Triaxial shear test: (a) machine and (b) results

Table 1 Mineral composition of a soil sample collected from P-10

Mineral	Chemical formula	Composition (%)
Quartz	SiO_2	42
Micas (muscovite)	$KAl_2(AlSi_3O_{10})(OH)_2$	22
Clays (kaolinite)	$Al_2(Si_2O_5)(OH)_4$	17
Postassium Feld. (microcline)	$KAlSi_3O_8$	13
Anatase	TiO_2	2
Chlorites (clinochlore)	$(Mg, Fe^{2+})_5$ $Al((OH)_8/AlSi_3O_{10})$	2
Gypsum	$CaSO_4 \cdot 2H_2O$	1
Smectite (montmorillonite)	$(Na, Ca)_{0.33}(Al, Mg)_2$ $(Si_4O_{10})(OH)_2 \cdot nH_2O$	< limit detection

From a compilation of several tests, a range of parameters is defined and shown in Table 2. Including previous results from direct shear and undrained triaxial tests, the cohesion of the soils of Pucallpa ranges from 10 kPa to 100 kPa, while the friction angle ranges from 11° to 16°.

Table 2 Parameters of Pucallpa soils obtained through different tests

Parameter	Units	Minimum value	Maximum value	Average value
e_{v0}	(–)	0.55	1.20	0.875
C_c	(–)	0.078	0.197	0.138
C_r	(–)	0.009	0.031	0.020
c'	(kPa)	15	124	69.5
ϕ'	(°)	10.5	16	13.3

3. CONSTITUTIVE RELATIONS AND ASSESSMENT OF MODEL PARAMETERS

In this section, the constitutive relations are described and the required parameters to represent the elasto-plastic behavior of the soils from Pucallpa are evaluated.

The changes in the effective stress $\boldsymbol{\sigma}' = \{\sigma_{xx}\ \sigma_{yy}\ \sigma_{zz}\ \tau_{xy}\ \tau_{yz}\ \tau_{xz}\}$ are related with the strain changes $\boldsymbol{\varepsilon} = \{\varepsilon_{xx}\ \varepsilon_{yy}\ \varepsilon_{zz}\ \gamma_{xy}\ \gamma_{yz}\ \gamma_{xz}\}$ through

$$\Delta\boldsymbol{\sigma}' = \boldsymbol{D}\Delta\boldsymbol{\varepsilon} \tag{1}$$

where $\boldsymbol{D}$ represents the stiffness matrix that can be assessed through:

$$\boldsymbol{D} = \boldsymbol{D}_e - \frac{\boldsymbol{D}_e\,\boldsymbol{g}_P\,\boldsymbol{g}_F^T\,\boldsymbol{D}_e}{\boldsymbol{g}_F^T\,\boldsymbol{D}_e\,\boldsymbol{g}_P + H} \tag{2}$$

in which $\boldsymbol{D}_e$ is the elastic stiffness matrix; $\boldsymbol{g}_F = \partial F/\partial\boldsymbol{\sigma}'$ is the gradient of the yield function (F); $\boldsymbol{g}_P = \partial P/\partial\boldsymbol{\sigma}'$ is the gradient of the plastic potential function (P); and H is the hardening/softening parameter. Observe that for elastic models, $\boldsymbol{D} = \boldsymbol{D}_e$.

Under elastic and isotropic behavior, two parameters define the elastic stiffness matrix: the bulk (K) and the shear (G) moduli. In a linear elastic model, such parameters are constant. On the other hand, in a non-linear elastic model (NLE), both parameters are stress dependent and given by

$$K_{\text{NLE}} = \frac{v\,p'}{\kappa} \tag{3}$$

$$G_{\text{NLE}} = \frac{3(1-2v)}{2(1+v)}\frac{(1+e)\,p'}{\kappa} \tag{4}$$

where κ is the swelling index (proportional to the recompression index), v is the Poisson ratio and p' is the mean effective stress.

Besides the soil elastic parameters, a yield surface must be adopted to identify the beginning of plastic deformations. In general, the yield surface is given as a convex mathematical function and its definition depends on the adopted constitutive model and the kind of application. For bearing capacity analyses, the yield surface is usually given by a shear failure function based on the frictional character of soils, for example adopting the Mohr-Coulomb or Drucker-Prager models. However, such models cannot take into account the occurrence of plastic deformations owing to the application of hydrostatic loadings, as it is observed in fine-grained soils. On the other hand, critical state models based on Cam clay formulations are capable of representing such soil behavior, but they significantly overestimate the shear failure stresses in overconsolidated soils (Potts and Zdravkovic 1999). Thus, "Cap models" (Sandler *et al.* 1976; Resende *et al.* 1985) emerged combining the capabilities of both frictional and critical state models through the adoption of two yield surfaces. In this study, we adopted the Modified Drucker-Prager/Cap model (MDPC) into the software ABAQUS. In this model, the yield function has three principal segments: a pressure dependent Drucker-Prager shear failure segment is given as:

$$F_s = \frac{q}{g} - p'\tan\beta - d = 0 \tag{5}$$

a compression cap segment:

$$F_c = \sqrt{(p'-p_a)^2 + \left(\frac{Rq/g}{1+\alpha-\alpha/\cos\beta}\right)^2} - R(d + p_a\tan\beta) = 0 \tag{6}$$

and a smooth transition segment between the shear failure surface and the cap:

$$F_t = \sqrt{(p'-p_a)^2 + \left[\frac{q}{g} - \left(1-\frac{\alpha}{\cos\beta}\right)(d + p_a\tan\beta)\right]^2} - \alpha(d + p_a\tan\beta) = 0 \tag{7}$$

where q is the von Mises or deviatoric stress; and β and d are model parameters related to the friction angle and the cohesion, respectively. R is a parameter that controls the shape of the cap, α is a parameter adopted to define a smooth transition between the shear failure and the compression cap segments, and p_a is a parameter that controls the cap evolution as follows:

$$p_a = \frac{p_b - Rd}{1 + R\tan\beta} \tag{8}$$

where p_b is the preconsolidation pressure that controls isotropic hardening/softening as a function of the plastic volumetric strain (ε_v^p) as it follows:

$$p_b = p_0\,e^{\left(\frac{1+e_0}{\lambda-\kappa}\right)\varepsilon_v^p} \tag{9}$$

where λ is the slope of the normal compression line, and p_0 and e_0 are initial values of the preconsolidation pressure and the void ratio, respectively.

The variable g used in Eqs. (5) and (6) is a function used to control the shape of the yield surface in the deviatoric plane and is defined as:

$$g = \frac{2K}{1 + K + (1-K)\left(\frac{r}{q}\right)} \tag{10}$$

where r is the third stress invariant and K is a material parameter that defines the ratio of the yield stress in triaxial tension to the yield stress in triaxial compression. The values of K must be

defined in such form that the yield surface remains convex, therefore $0.778 \le K \le 1$. The lower value is given to reproduce yielding surfaces close to the projection of the Mohr Coulomb pyramid over the deviatoric plane. On the other hand, setting $K = 1$ causes the yield surface to be independent of the third stress invariant and the projection of the yield surface on the deviatoric plane becomes a circle (Helwany 2007). Figure 8 shows the proyection of the yield surfaces of the MDPC model in the meridional and the deviatoric planes.

Finally, to complete the formulation of the model, it is necessary to define plastic potential functions (P). Associated flow rules are assumed in the deviatoric plane and in the cap region of the meridional plane, as follows:

$$P_c = \sqrt{(p' - p_a)^2 + \left(\frac{Rq/g}{1+\alpha-\alpha/\cos\beta}\right)^2} \tag{11}$$

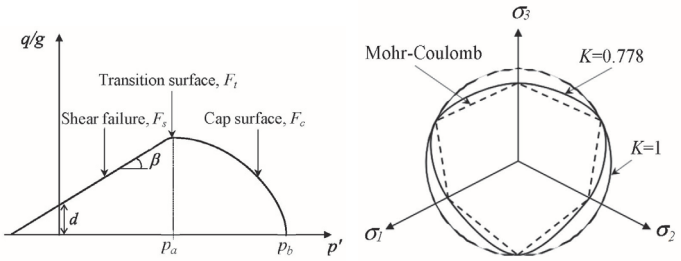

Fig. 8 Yield surfaces in (a) the meridional plane and in (b) the deviatoric plane (adapted from ABAQUS 2020)

However, in the failure surface and in the transition region, the plastic function is non-associative in order to avoid the drawbacks of frictional models. The elliptical flow potential surface is given as

$$P_s = \sqrt{[(p' - p_a)\tan\beta]^2 + \left(\frac{q/g}{1+\alpha-\alpha/\cos\beta}\right)} \tag{12}$$

More details about the MDPC model can be found in the literature (Helwany 2007).

During field and laboratory data acquisition, most investigation reports adopt the one-dimensional consolidation (C_c and C_r) and the shear strength (c' and ϕ') parameters as shown in Table 2. However, to use the MDPC model, λ, κ, β, and d must be assessed. The consolidation parameters are related as

$$\lambda = \frac{C_c}{2.303}, \quad \kappa = \frac{C_r}{2.303} \tag{13}$$

For 3D analyses, the shear strength parameters of the MDPC model are related to the Mohr-Coulomb parameters obtained in triaxial tests as follows

$$\tan\beta = \frac{6\sin\phi'}{K(3-\sin\phi')}; \quad d = \frac{6\,c'\cos\phi'}{(3-\sin\phi')} \tag{14}$$

while for plane strain conditions, the shear strength parameters of the MDPC model are assessed as:

$$\tan\beta = \frac{\sqrt{3}\sin\phi'}{K\left(1+\frac{1}{3}\sin\phi'\right)}; \quad d = \frac{\sqrt{3}\cos\phi'\,c'}{\sqrt{1+\frac{1}{3}\sin\phi'}} \tag{15}$$

Besides those parameters, initial conditions of the soil such as the initial stress state (p') and the corresponding preconsolidation pressure (p_0) and void ratio (e_0) must be given as input data.

A reasonable approach for the assessment of the in-situ stress is to consider that the vertical stress is the major principal one, and the two horizontal effective stresses are equivalent to the minor principal one. Then, the vertical and horizontal stresses can be assessed as follows:

$$\sigma'_v = \gamma z, \quad \sigma'_h = K_0\,\sigma'_v \tag{16}$$

where z is the depth and K_0 is the at-rest earth pressure coefficient.

The magnitude of K may be directly measured through special testing equipment either in the laboratory or in the field. Alternatively, empirical correlations can be used including stress history, soil index parameters and in-situ test results (Jaky 1948; Schmidt 1967; Kulhawy and Mayne 1990; Mesri and Hayat 1994). Many factors can affect the in-situ state stress in soils such as overconsolidation, aging or chemical bonding. However, owing to glaciation, erosion, desiccation, excavation and ground water fluctuations, the soil overconsolidation is the most relevant factor in geotechnical engineering. Based on several tests in laboratory, Kulhawy and Mayne (1990) suggested a relation for overconsolidated clays as a function of the mobilized friction angle:

$$K_0 = (1-\sin\phi')\,\mathrm{OCR}^{\sin\phi'} \tag{17}$$

where OCR is the overconsolidation ratio defined as the ratio of the maximum stress experienced by the soil to the current stress. Observe that for those normally consolidated soils, Eq. (17) is simplified into Jaky's empirical formula. At high values of OCR, the soil can present lateral stresses greater than the vertical stress ($K_0 > 1$) because, at some point in its geological history, the soil was under a greater vertical stress than its current one. Moreover, for the same material, overconsolidated soils are in general stiffer than normally consolidated soils (OCR = 1) and can present softening with reduction in the strength parameters during shearing (Summersgill 2014).

The value of OCR can be obtained through some correlations; for example, Stas and Kulhawy (1984) suggested the following:

$$\mathrm{OCR} = \frac{p_{atm}}{\sigma'_v} 10^{(1.11-1.62\mathrm{LI})} \tag{18}$$

in which p_{atm} is the atmospheric pressure and LI is the liquidity index given as:

$$\mathrm{LI} = \frac{w - \mathrm{LL} + \mathrm{PI}}{\mathrm{PI}} \tag{19}$$

where w is the natural water content. Considering Eq. (19), the OCR for the soils of Pucallpa varies between 2 and 8.

Moreover, if N values from standard penetration tests (SPT) are available and where $cf = 0.85$ (correction factor that depends on the used equipment), the preliminary overconsoli-

dation ratio for cohesive soils can be obtained as (Mayne and Kemper 1988):

$$\mathrm{OCR} = \frac{p_{atm}}{\sigma'_v} 0.58\ cf \times N \tag{20}$$

Taking into account Eq. (20), the OCR for soils located at depths ranging from 1 to 5 meters varies between 3 and 10. There are other empirical equations for undrained behavior of clay with varying degrees of overconsolidation (Anantanasakul and Roth 2018).

Once the initial stresses are assessed, the mean effective stress is obtained through:

$$p' = \frac{\sigma'_v + 2\sigma'_h}{3} \tag{21}$$

Then, the initial preconsolidation pressure (p_0) can be assessed as follows:

$$p_0 = p' \,\mathrm{OCR} \tag{22}$$

and finally, the initial void ratio (e_0) is assessed as:

$$e_0 = e_{v0} - (\lambda - \kappa) \ln p_0 - \kappa \ln p' \tag{23}$$

where e_{v0} is the initial void ratio at the virgin consolidation line considering p' = 1 kPa.

4. ANALYSES OF THE BEARING CAPACITY AND SETTLEMENT OF A SHALLOW FOUNDATION

Theoretical relations based on total or effective stress concepts have been proposed to assess the ultimate bearing capacity of shallow foundations. For example, for strip foundations (or strip footings) of width (B) and located at a depth (D), Terzaghi (1943) defined the ultimate bearing capacity (q_u) in the form:

$$q_u = \gamma D N_q + c' N_c + 0.5 \gamma B N_\gamma \tag{24}$$

where N_q, N_c, and N_r are bearing capacity factors used to represent the influence of the overburden stress, the soil cohesion and the unit weight, respectively. Such factors can be assessed as functions of the friction angle as follows:

$$N_q = e^{\pi \tan \phi'} \tan^2 \left(45° + \frac{\phi'}{2} \right) \tag{25}$$

$$N_c = (N_q - 1) \cot \phi' \tag{26}$$

$$N_r = (N_q - 1) \tan(1.4\, \phi') \tag{27}$$

Observe that in those equations, Terzaghi considers constant shear strength parameters (c' and ϕ') defined in terms of effective stresses. Through several CIU tests carried out on Kaolinite and Silty clays, Murthy *et al.* (1981) showed that Mohr-Coulomb strength envelopes on effective stress basis are uniquely defined, independent of OCR and the past maximum pressure (p_0). Those authors also demonstrated that unique effective stress parameters (c' and ϕ') equal to the peak stress values are observed at pre-peak strains even before the failure stress conditions are reached. However, no such uniqueness is found with respect to total stress. According to Murthy *et al.* (1981), the Mohr-Coulomb envelopes plotted in terms of total stresses are nonlinear, with the angle of shearing resistance increasing with OCR. Despite this fact, the total stress concept is still present in several engineering applications (Whitman 1960), particularly when high loading rates do not allow the pore pressure dissipation. Skempton (1951), for example, suggested that under undrained conditions, the friction angle is null; therefore, N_q and N_γ are equal to unity and zero, respectively. Thus, Eq. (24) is reduced to the simple form:

$$q_u = \gamma D + s \cdot N_c \tag{28}$$

where s represents the undrained shear strength of the clay, and the factor N_c is evaluated as a function of B and D in strip footings according to:

$$N_c = 5 \left(1 + 0.2 \frac{D}{B} \right) \tag{29}$$

Now, it is possible to compare the results of Eqs. (24) and (28) considering the parameters listed in Table 2, and B = 0.6 m and D = 1.5 m for a given footing. For the assessment of s, we use the *UCS* values shown in Fig. 2(b). In general, the undrained shear strength is approximated as half of *UCS*. Considering the depth of 1.5 m, we observe values of *UCS* ranging from 100 to 400 kPa which provide s values of 50 and 200 kPa, respectively. With those limits in Eq. (28), we obtain ultimate bearing capacities ranging from 400 to 1,525 kPa. That significant difference in values can be attributed to the different overconsolidated ratios at each place where the field tests were performed. However, Terzaghi's solution is unique and provides an ultimate bearing capacity of 783.6 kPa.

typically, for normally consolidated clays, the undrained shear strength is lower than the drained strength owing to increases in pore pressure and decreases in effective stress during the undrained shear. That is observed when we compare the bearing capacity using the lowest *UCS* value in Skempton's equation (400 kPa) and that using Terzaghi's equation (784 kPa). On the other hand, for very heavily overconsolidated clays, the undrained strength is greater than the drained strength owing to negative pore pressures which increase the effective stress during the undrained shear. That can explain why the ultimate bearing capacity using the highest *UCS* value in Skempton's equation (1,525 kPa) is almost twice the value obtained using Terzaghi's equation. Therefore, using the undrained shear strength may not be conservative in long-term analyses, overestimating the ultimate bearing capacity of overconsolidated clays (Henkel and Skempton 1954; Duncan *et al.* 2014; Bahmyari 2018).

Besides theoretical solutions, numerical ones in terms of effective stress are performed in this study. Figure 9 shows the geometry and the finite element mesh used in the numerical tests. Owing to symmetry, only half of the problem is simulated. The quadrilateral elements adopt quadratic interpolation for displacements. In total, the mesh has 7,000 elements with 9-point Gauss integration and 7,171 nodes.

The material properties are shown in Table 3. Most parameters were obtained through correlations and data listed in Table 2. The soil mechanical behavior is represented through

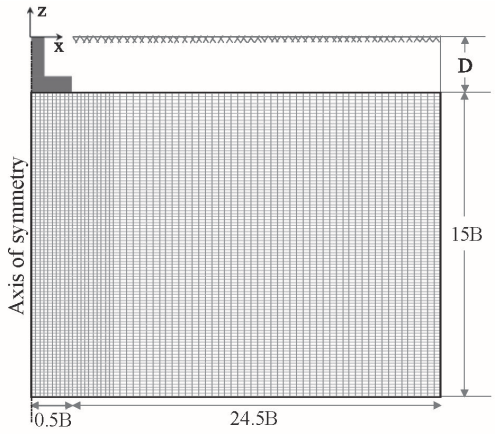

Fig. 9 Model geometry and mesh for numerical tests

Table 3 Parameters for the MDPC model adopted in the simulations

Parameter	Symbol	Units	Value
Void ratio at unit pressure	e_{v0}	(–)	0.875
Unit weight	γ	(kN/m^3)	17.0
Slope of the normal compression line	λ	(–)	0.06
Slope of the swelling line	κ	(–)	0.009
Correlated friction angle	β	(°)	26.85
Correlated cohesion	d	(kPa)	116.0
Model parameter	R	(–)	0.2
Model parameter	α	(–)	0.05
Model parameter	K	(–)	0.778

the MDPC model. The simulations are performed assuming drained conditions and different values of OCR (1, 2, 3, 5, and 10). Such OCR values are analysed because of uncertainties in the assessment of that parameter and in order to check its impact on the results.

The initial conditions are assessed through Eqs. (3), (4), (16), (17), (21), (22), and (23). Regarding the boundary conditions, the horizontal displacements are restricted at $x = 0$ and $x = 25B$. At the bottom of the model, the vertical displacements are restricted. Over the top of the model, from $x = 0$ to $x = 0.5B$, an incremental vertical displacement is applied until it reaches 1 m. Such condition is imposed in order to represent the settlement of a rigid footing.

The pressure-settlement curves are shown in Fig. 10. It can be noticed that the resultant curves are typical from stiff soils that develop sudden increases in settlement after reaching the ultimate bearing capacity. For comparison purposes, three vertical lines that represent the ultimate bearing capacities obtained through the theoretical solutions are also shown in that figure. One of them represents Terzaghi's solution and the other two correspond to Skempton's solutions for the lowest (Skempton 1) and highest (Skempton 2) undrained shear strengths considered. The results indicate that, independently of OCR, all numerical solutions predict ultimate bearing capacities similar to that obtained through the theoretical solution of Terzaghi. That indicates that under drained conditions, a general shear failure mechanism occurs in the shallow foundation, following the main assumption of Terzaghi's solution. Figure 10 also shows that Skempton's solutions represent minimum and maximum limits for the ultimate bearing capacity.

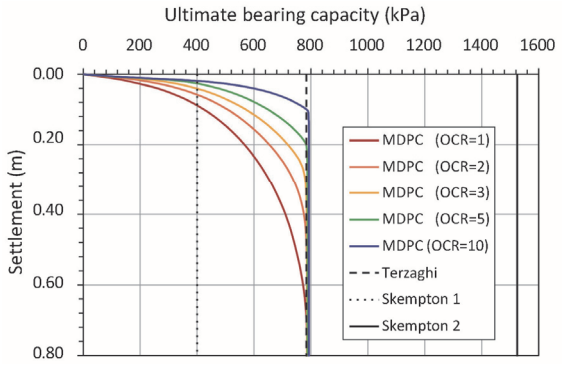

Fig. 10 Results considering different approaches for the bearing capacity

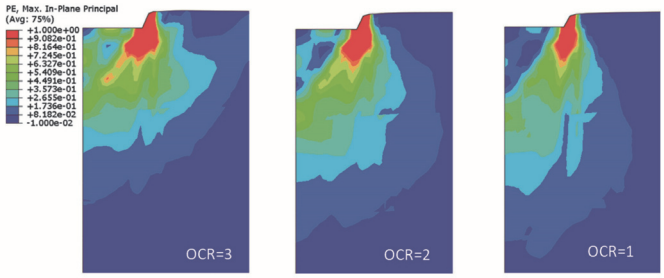

Fig. 11 Maximum plastic strain obtained for three simulation tests (mesh deformed by a factor of 0.1)

Figure 11 shows contour plots of the maximum value of the principal plastic strain (PE) at the end of three tests (OCR = 3, 2, and 1). These results confirm that general shear failure modes develop in the soil foundation.

From Fig. 10, it is also observed that the pressure-settlement curves develop as a function of the given OCR. As lower OCR values are adopted, less stiff is the soil; therefore, the settlements are higher when the soil reaches the ultimate bearing capacity. For example, the minimum settlement (100 mm) is obtained in the simulation of an overconsolidated soil with OCR = 10. In turn, the maximum settlement (690 mm) is reached when the soil is normally consolidated. The considerable difference in settlements between both results is explained not only by the different soil stiffness but also by the occurrence of plastic deformations. At higher values of OCR, the cap surface is more distant of the initial stress state and therefore, the triggered stress paths will reach such surface later. On the other hand, in soils normally consolidated, the cap surface is close to the initial stress state, and plastic volumetric deformations may occur sooner, enabling the highest settlements. Figure 12 shows the final preconsolidation pressures (p_b) obtained for the simulations with OCR = 10 and 1. It can be noticed that for the overconsolidated soil, the initial value of 516 kPa is increased up to 646 kPa, but such increase is concentrated at certain region below the footing. The preconsolidation pressure is also increased in the normally consolidated soil, but in this case, the region that suffers hardening is bigger and deeper than that in the overconsolidated soil.

Those results call the attention over the allowable settlements of shallow foundations, particularly resting over clays with the features of the soils of Pucallpa. Skempton and Macdonald

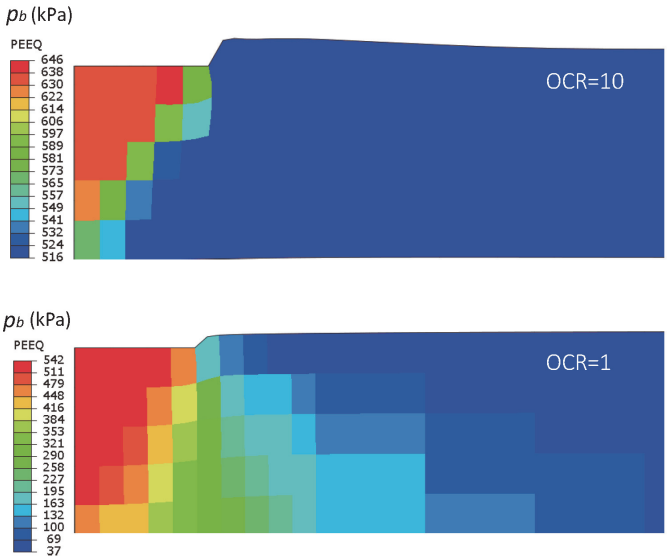

Fig. 12 Preconsolidation pressure for two simulation tests

(1956) suggested that the maximum settlements of continuous foundations resting over clays must be limited to 125 mm in order to avoid damage in buildings. Then, considering two critical values as 50 and 100 mm, the safe bearing capacity (q_{safe}) at each simulation can be obtained by the intersection of horizontal lines (with such allowable settlements) and the corresponding pressure-settlement curve, as it is shown in Fig. 13.

Then, some correlations between OCR and the safe bearing capacity can be found taking into account the allowable settlement as shown in Fig. 14. These results demonstrate that for a given maximum settlement, the safe bearing capacity is minimum for normally consolidated soils and significantly higher for overconsolidated soils. For example, considering an allowable settlement of 25 mm, the ultimate bearing capacity is approximately 500 kPa for a soil with OCR = 10, while for a normally consolidated soil, such capacity is 200 kPa. This last value shows that depending on the allowable settlement, the ultimate bearing capacity assessed under drained conditions can provide lower values than those assessed by the Skempton's solution (400 kPa) with an undrained shear strength. On the other hand, if we assume a maximum settlement of 100 mm, we

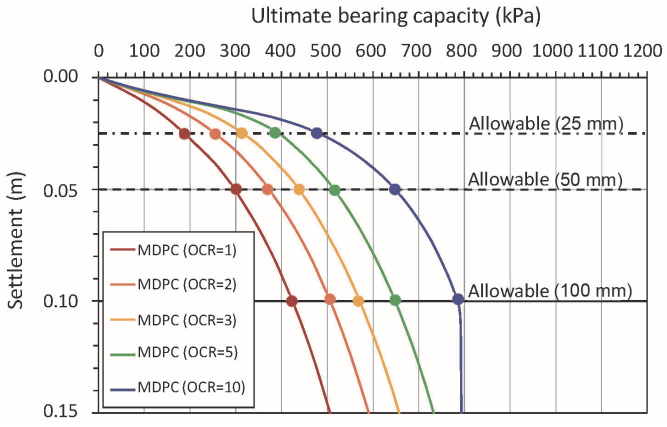

Fig. 13 Bearing capacities and allowable settlements for soils with different OCR values

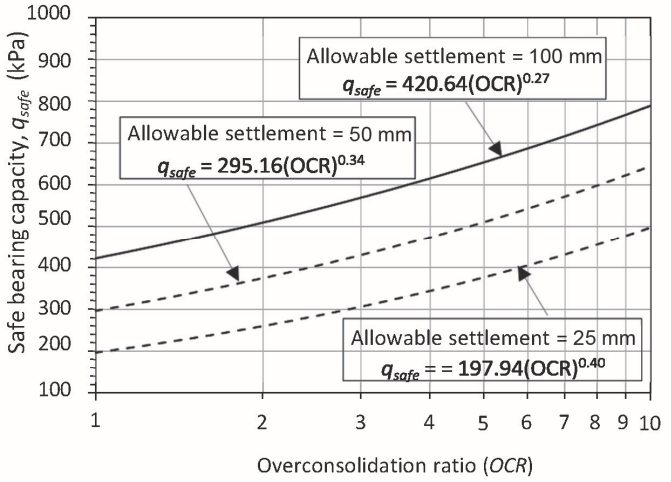

Fig. 14 Correlation between OCR and the allowable bearing capacity of soils of Pucallpa

can notice that the ultimate bearing capacity is close to that of Terzaghi's solution, but only for overconsolidated soils with OCR ≥ 10.

CONCLUSIONS

This study is focused on two main aspects. One is the characterization of Pucallpa's soils considering field and laboratory tests, and the other is the assessment of its ultimate bearing capacity using numerical and theoretical solutions. Through the analyses of the collected data, the soils of Pucallpa were classified as medium stiff to very stiff clays. Moreover, these soils presented different levels of overconsolidation. That can be explained by the occurrence of transport and accumulation of sediments as well as erosion processes, typical from the Amazon plain. Owing to such characteristics, the mechanical behavior of those soils was represented by the Modified Drucker-Prager/CAP (MDPC) considering not only its shear strength but also its compaction. Then, numerical simulations of a strip footing resting over soils with different OCR were performed assessing their bearing capacity assuming drained loadings. In addition, we computed the ultimate bearing capacities considering some drained and undrained theoretical solutions, typically adopted in the design of shallow foundations.

From the found results, the following conclusions can be highlighted:

1. All numerical results forecasted an ultimate bearing capacity similar to that found through Terzaghi's solution. Those results prove that under drained loadings, shallow foundations resting over stiff clays can trigger a general shear failure mode only dependent on the cohesion and friction angles adopted.
2. The ultimate bearing capacity was also computed through Skempton's solution based on undrained shear strength. Considering limit values of *UCS* found at different places of Pucallpa, we assessed lower and higher ultimate bearing capacities than those found under drained conditions. These results show that the undrained shear strength does not necessarily provide the lowest bearing capacity. Actually, undrained conditions provide conservative solution

only in the case of normally consolidated clays. However, for overconsolidated soils, the use of undrained shear strength can provide unconservative solutions.

3. Through the numerical results, we also showed that for design purposes, it is necessary to evaluate both the bearing capacity and the settlements triggered by the foundation. Considering the pressure-settlement curves at each simulation and critical settlements, it was possible to determine some relationships between the overconsolidation ratio and safe bearing capacities for the soils of Pucallpa. These results demonstrate that the bearing capacity and the soil settlement must be evaluated together for an appropriate design of shallow foundations, particularly in overconsolidated clays.

ACKNOWLEDGMENTS

The authors would like to thank the Geotechnical Laboratory of the Universidad de Lima for the support and interest in this study. Acknowledgment also goes to Pablo Valderrama Pablo for collecting a series of samples in the city of Pucallpa and Andrei Dominguez to assist in a series of laboratory experiments.

FUNDING

This research was supported by the Instituto de Investigación Científica (IDIC) of the Universidad de Lima.

DATA AVAILABILITY

This study does not generate new data and/or new computer codes.

CONFLICT OF INTEREST STATEMENT

The authors state that there are no financial interests or personal relationships that might influence the work reported in this paper.

REFERENCES

ABAQUS (2020). *ABAQUS Documentation*, Dassault Systemes Simulia Corp: Providence, RI, USA.

Ajayi, L. and Balogum, L. (1988). "Penetration testing in tropical lateritic and residual soils – Nigerian experience." *Proc., 1st International Symposium on Penetration Testing, ISOPT-1*, Orlando, **1**, 315-328. https://doi.org/10.1016/0148-9062(90)95080-k

Alva, J. (2013). "Estudios geotécnicos en la ciudad de pucallpa," *Universidad Nacional del Ingeniería*, 132 (in Spanish). http://www.jorgealvahurtado.com/files/EstudiosGeotecnicosPucallpa.pdf. Accessed 26 Frebrery 2021

Alva, J. (2018). "Características Geotécnicas de los suelos de la selva peruana," *Proc., XX CONIC: Congreso Nacional de Ingeniería Civil*, Lima, Peru, 131. http://www.jorgealvahurtado.com/files/Caracteristicasgeotecnicassuelosselva.pdf

Anantanasakul, P. and Chanraksmey, R. (2018). "Undrained behavior of silt-clay transition soils with varying degrees of overconsolidation," *Journal of GeoEngineering*, **13**(1), 1-12. https://doi.org/10.6310/jog.201803_13(1).1

Bahmyari, H. (2018). *Shear Strength Characteristics and Failure Mechanism of Slopes in Overconsolidated Soils of Nebraska*, Civil Engineering Theses, Dissertations, and Student Research, University of Nebraska.

Biot, M.A. (1941). "General theory of three-dimensional consolidation," *Journal of Applied Physics*, **12**(2), 155-164. https://doi.org/10.1063/1.1712886

Budhu, M. (2012). "Design of shallow footings on heavily overconsolidated clays," *Canadian Geotechnical Journal*, **49**(2), 184-196. https://doi.org/10.1139/t11-093

Bustamante, A. and Alva, J. (1995). "Características Geotecnicas Del Suelo De Iquitos, Peru," *Proc., 10th Panamerican Conference-Soil Mechanics and Foundation Engineering*, Guadalajara, Mexico, 29-42.

Camacho, J. and Reyes, O. (2005). "Aplicación del modelo cam-clay modificado en arcillas reconstituidas del la sabana de Bogotá," *Revista Ingeniería de Construcción*, **20**, 159-160.

Chakraborty, D. and Jyant, K. (2013). "Dependency of Nγ on footing diameter for circular footings," *Soils and Foundations*, **53**(1), 173-180. https://doi.org/10.1016/j.sandf.2012.12.013

Chen, Z., Pengpeng, N., Yifeng, C. and Guoxiong, M. (2020). "Plane-strain consolidation theory with distributed drainage boundary," *Acta Geotechnica*, **15**(2), 489-508. https://doi.org/10.1007/s11440-018-0712-z

Chwała, M. and Wojciech, P. (2020). "Evaluation of shallow foundation bearing capacity in the case of a two-layered soil and spatial variability in soil strength parameters," *Plos One*, **15**(4), 1-23. http://dx.doi.org/10.1371/journal.pone.0231992

Davis, E.H. and Raymond, G.P. (1965). "A non-linear theory of consolidation," *Géotechnique*, **15**(2), 161-173. https://doi.org/10.1680/geot.1965.15.2.161

Díaz, Z. (2000). *Génesis, morfologia y clasificación de algunos suelos de Pucallpa,* Universidad Nacional Agraria La Molina, Lima, Perú.

Duncan, J.M., Wright, S.G., and Brandon, T.L. (2014). *Soil Strength and Slope Stability*, 2nd Ed., John Wiley & Sons, Inc.

Foye, K.C., Basu, P., and Prezzi, M. (2008). "Immediate settlement of shallow foundations bearing on clay," *International Journal of Geomechanics*, ASCE, **8**(5), 300-310. https://doi.org/10.1061/(ASCE)1532-3641(2008)8:5(300)

Gibson, R.E. and Mcnamee, J. (1963). "A three-dimensional problem of the consolidation of a semi-infinite clay stratum," *Quarterly Journal of Mechanics and Applied Mathematics*, **16**(1), 115-127. https://doi.org/10.1093/qjmam/16.1.115

Goh, A., Zhang, R., Wang, W., Wang, L., Liu, H. and Zhang, W. (2020). "Numerical study of the effects of groundwater drawdown on ground settlement for excavation in residual soils," *Acta Geotechnica*, **15**(6), 1259-1272. https://doi.org/10.1007/s11440-019-00843-5

Hara, A., Ohta, T., Niwa, M., Tanaka, S., and Banno, T. (1974). "Shear modulus and shear strength of cohesive soils," *Soils and Foundations*, **14**(3), 1-12. https://doi.org/10.3208/sandf1972.14.3_1

Helwany, S. (2007). *Applied Soil Mechanics with ABAQUS Applications*, John Wiley & Sons, New Jersey.

Henkel, D.J. and Skempton, A.W. (1954). "A landslide at jack-

field, shropshire, in a heavily over-consolidated clay." *Géotechnique*, **5**(2), 131-137. https://doi.org/10.1680/geot.1955.5.2.131

Huang, W., Fityus, S., Bishop, D., Smith, D., and Sheng, D. (2006). "Finite-element parametric study of the consolidation behavior of a trial embankment on soft clay," *International Journal of Geomechanics*, ASCE, **6**(5), 328-341. https://doi.org/10.1061/(ASCE)1532-3641(2006)6:5(328)

Jaky, J. (1948). "Pressure in silos," *Proc., 2nd International Conference on Soil Mechanics and Foundation Engineering*, Rotterdam, Nederland, **1**, 103-107.

Kawa, M. and Pula, W. (2019). "3D bearing capacity probabilistic analyses of footings on spatially variable c-phi soil," *Acta Geotechnica*, **15**, 1453-1466. https://doi.org/10.1007/s11440-019-00853-3

Kulhawy, F.H. and Mayne, P.W. (1990). *Manual on Estimating Soil Properties for Foundation Design*, EPRI Report EL-6800, Cornell University, Ithaca, New York.

Ledesma, O. (2007). *Calibración del Cam Clay para los suelos del postpampeano*, Dissertation, Facultad de Ingenieria, Universidad de Buenos Aires, (1), 18 (in Spanish). http://materias.fi.uba.ar/6408/Ledesam_Sfriso_revisado2.pdf

Lee, P.K.K., Xie, K.H., and Cheung, Y.K. (1992). "A study on one-dimensional consolidation of layered systems," *International Journal for Numerical and Analytical Methods in Geomechanics*, **16**(11), 815-831. https://doi.org/10.1002/nag.1610161104

Liyanapathirana, D.S., Carter, J.P., and Airey, D.W. (2009). "Drained bearing response of shallow foundations on structured soils," *Computers and Geotechnics*, **36**(3), 493-502. https://doi.org/10.1016/j.compgeo.2008.04.004

Lukić, I., Maja, P. and Vlasta, S-N. (2020). "Numerical modeling of settlements for shallow foundations on layered soils," *E-Zbornik*, **10**(19), 47-62. https://doi.org/10.47960/2232-9080.2020.19.10.47

Mandel, J. (1953). "Consolidation des sols (Étude Mathématique)," *Géotechnique*, **3**(7), 287-299. https://doi.org/10.1680/geot.1953.3.7.287

Mayne, P., and Kemper, J. (1988). "Profiling OCR in stiff clays by CPT and SPT," *Geotechnical Testing Journal*, **11**(2), 139-147. https://doi.org/10.1520/GTJ10960J

Mesri, G. and Hayat, T.M. (1994). "The coefficient of earth pressure at rest: Reply," *Canadian Geotechnical Journal*, **31**(5), 791-793. https://doi.org/10.1139/t94-092

Meyerhoff, G. (1951). "The ultimate bearing capacity of foundations," *Géotechnique*, **2**(4), 301-332. https://doi.org/10.1680/geot.1951.2.4.301

Potts, M.D. and Zdravkovic, L. (1999). *Finite Element Analysis in Geotechnical Engineering: Theory*, Thomas Telford Ltd., Heron Quay, London.

Quevedo, R.J. (2012). *Three-Dimensional Analysis of Hydromechanical Problems in Partially Saturated Soils*. Pontifical University of Rio de Janeiro (in Portuguese).

Rachdi, S., Jahangir, E., Tijani, M., and Serratrice, J.-F. (2019). "Critical state constitutive models and shear loading of overconsolidated clays with deviatoric hardening," *Studia Geotechnica et Mechanica*, **41**(4), 247-262. https://doi.org/10.2478/sgem-2019-0024

Radhika, B., Krishnamoorthy, A., and Rao, A. (2020). "A review on consolidation theories and its application," *International Journal of Geotechnical Engineering*, **14**(1), 9-15. https://doi.org/10.1080/19386362.2017.1390899

Ramírez, E., Valencia, M. and Vela, J. (2018). "Génesis, morfología, clasificación y susceptibilidad de suelos de la parte media de la cuenca del río Abujao Región Ucayali," *Anales Científicos*, **79**(2), 368-376. https://doi.org/10.21704/ac.v79i2.1249

Resende, L. and Martin, J.B. (1985). "Formulation of drucker-prager cap model," *Journal of Engineering Mechanics*, ASCE, **111**(7), 855-881. https://doi.org/10.1061/(ASCE)0733-9399(1985)111:7(855)

Rigo, M., Barboza, R., Bressani, L., Damiani, A., and Moraes, R. (2006). "The residual shear strength of tropical soils," *Canadian Geotechnical Journal*, **43**(4), 431-447. https://doi.org/10.1139/t06-015

Sandler, I., Baladi, G. and DiMaggio, F. (1976). "Generalized cap model for geological materials," *Journal of the Geotechnical Engineering Division*, ASCE, **102**(7), 683-697. https://doi.org/10.1061/AJGEB6.0000293

Schmidt, B. (1967). "Lateral stresses in uniaxial strain," *Geoteknisk Institut (The Danish Geotechnical Institute)*, **23**, 5-12.

Schneider-Muntau, B. and Bathaeian, I. (2018). "Simulation of settlement and bearing capacity of shallow foundations with soft particle code (SPARC) and FE," *International Journal on Geomathematics*, **9**(2), 359-375. https://doi.org/10.1007/s13137-018-0109-z

Skempton, A.W. (1985). "Residual strength of clays in landslides, folded strata and the laboratory," *Geotechnique*, **35**(1), 3-18. https://doi.org/10.1680/geot.1985.35.1.3

Skempton, A.W. and Macdonald, D.H. (1956). "The allowable settlements of the buildings," *Proc., Institution of Civil Engineers*, **5**(6), 727-768. https://doi.org/10.1680/ipeds.1956.12202

Stas, C.V. and Kulhawy, F.H. (1984). *Critical Evaluation of Design Methods for Foundations Under Axial Uplift and Compression Loading*, *Final Report*, Cornell Univ., Ithaca, NY (USA), Geotechnial Engineering Group, United States of America.

Summersgill, F. (2014). *Numerical Modelling of Stiff Clay Cut Slopes with Nonlocal Strain Regularisation*, Dissertation, Imperial College London.

Sun, W., Chen, Q. and Ostien, J.T. (2014). "Modeling the hydro-mechanical responses of strip and circular punch loadings on water-saturated collapsible geomaterials," *Acta Geotechnica*, **9**(5), 903-934. https://doi.org/10.1007/s11440-013-0276-x

Tang, Y., Taiebat, H.A., and Senetakis, K. (2017). "Effective stress based bearing capacity equations for shallow foundations on unsaturated soils," *Journal of GeoEngineering*, **12**(2), 59-64. https://doi.org/10.6310/jog.2017.12(2).2

Terzaghi, K. (1943). *Theoretical Soil Mechanics*. John Wiley and Sons, London. https://doi.org/10.1002/9780470172766

Terzaghi, K. and Peck, R. (1967). *Soil Mechanics in Engineering Practice*, John Wiley, New York.

Vesic, A.S. (1973). "Analysis of ultimate loads of shallow foundations," *Journal of the Soil Mechanics and Foundations*, **99**(1), 45-73. https://doi.org/10.1061/JSFEAQ.0001846

Whitman, R.V. (1960). "Discussion on shear strength of undisturbed cohesive soils, Session 4," *Proc., Research Conference on Shear Strength of Cohesive Soils*, ASCE, pp. 1067-1092.